HHS Public Access

Author manuscript

Mol Reprod Dev. Author manuscript; available in PMC 2022 July 01.

Published in final edited form as:

Mol Reprod Dev. 2021 July ; 88(7): 482–489. doi:10.1002/mrd.23473.

Generation and analysis of *Prss28* and *Prss29* deficient mice using CRISPR-Cas9 genome-editing

Pramod Dhakal[1], **Thomas E. Spencer**[1,2]

[1]Division of Animal Sciences, Gynecology and Women's Health, University of Missouri, Columbia, MO, USA

[2]Department of Obstetrics, Gynecology and Women's Health, University of Missouri, Columbia, MO, USA

Abstract

Glands of the uterus are essential for the establishment of pregnancy in mice and their products regulate embryo implantation and stromal cell decidualization critical for pregnancy establishment. Forkhead box A2 (FOXA2) is expressed specifically in the glands and a critical regulator of their differentiation, development and function. Progesterone and FOXA2 regulate members of a serine proteinase gene family (*Prss28* and *Prss29)*. Here, CRISPR-Cas9 genome-editing was used to create mice with a heterozygous or homozygous deletion of *Prss28* or/and *Prss29* to determine their biological roles in uterine function. Female mice lacking *Prss28* and *Prss29* or both developed normally and were fertile without alterations in uterine histoarchitecture, uterine gland number, or and gene expression. Thus, Prss28 and Prss29 are dispensable for female fertility and do not impact endometrial gland development or uterine function mice.

Keywords

Prss28 ; *Prss29* ; uterus; gland

1 INTRODUCTION

Uterine glands and, by inference, their secretions regulate embryo implantation and pregnancy establishment in mice (Kelleher, Milano-Foster, Behura, & Spencer, 2018). Infertility in leukemia inhibitory factor (Lif) null mice and uterine gland knockout mice and sheep established the importance of the endometrial glandular epithelia (GE) and, by inference, their secretions and products for embryo implantation (Cooke et al., 2012; Filant & Spencer, 2013; Gray, Burghardt, Johnson, Bazer, & Spencer, 2002; Gray et al., 2001; Jeong et al., 2010; Stewart, 1994; Stewart et al., 1992). Recent evidence indicates that

Correspondence: Thomas E. Spencer, 920 East Campus Drive, 135 ASRC, Division of Animal Sciences, University of Missouri, Columbia, MO 65211, USA. Tel: +1 (573) 882-3467; spencerte@missouri.edu.

Conflict of interests

The authors have declared that no conflict of interest exists.

Data sharing and data availability

The data that support the findings of this study are available from the corresponding author upon reasonable request.

uterine glands impact stromal cell decidualization (Kelleher, Behura, et al., 2019; Kelleher, DeMayo, & Spencer, 2019; Kelleher et al., 2018; Kelleher et al., 2017). Additionally, uterine glands have direct connections to the developing placenta in mice (Arora et al., 2016; Yuan et al., 2018) and humans (Burton, Watson, Hempstock, Skepper, & Jauniaux, 2002). Thus, products and secretions of endometrial glands are hypothesized to control development and growth of embryo and placenta throughout pregnancy (Dhakal, Kelleher, Behura, & Spencer, 2020; Kelleher, DeMayo, et al., 2019).

In the uterus, FOXA2 is expressed specifically in the endometrial GE of mice (Filant, Lydon, & Spencer, 2014; Filant & Spencer, 2013; Jeong et al., 2010) and humans (Villacorte et al., 2013). Adult FOXA2 conditional knockout (cKO) mice lacked expression of LIF, a gland-specific factor induced by estrogen from the ovary on gestational day (GD) 4 (Bhatt, Brunet, & Stewart, 1991; J. R. Chen et al., 2000). LIF is critical for embryo implantation (Bhatt et al., 1991; Stewart et al., 1992) with pleiotropic effects on the uterine epithelium to regulate uterine receptivity (J. R. Chen et al., 2000; Fouladi-Nashta et al., 2005). In addition to *Lif*, a number of progesterone-induced genes expressed in the uterine glands (e.g., *Prss28*, *Prss29*) were not expressed in the uterus of adult FOXA2 cKO mice (Kelleher et al., 2018; Kelleher et al., 2017). Notably, ChIP-seq established that *Prss28* and *Prss29* have FOXA2 binding sites in their gene promoter/enhancer regions (Filant et al., 2014).

The *Prss28* and *Prss29* genes, also known as implantation serine proteinase 1 (Isp1) and 2 (Isp2), respectively, are within a tryptase cluster in chromosome 17 of mouse genome (Tang & Rancourt, 2005) and were initially hypothesized to have a biological role in embryo hatching (O'Sullivan, Rancourt, Liu, & Rancourt, 2001). Both genes are expressed specifically and abundantly in GE of the mouse uterus and induced by progesterone (O'Sullivan et al., 2004). Of note, expression of both genes starts about GD 5.5, correlating to when glands influence pregnancy establishment via effects on stromal cell decidualization (Kelleher, DeMayo, et al., 2019).

The objective here was to test the hypothesis that Prss28 and Prss29 have biological roles in uterine function to support establishment and maintenance of pregnancy. CRISPR-Cas9 genome-editing was used to generated mono- and bi-allelic deletions of *Prss28* and *Prss29* in mouse embryos. Studies were then performed to determine the effects of *Prss28* and *Prss29* deficiency on female fertility and uterine function.

2 Materials and methods

2.1 Animals

Animal procedures were approved by the Institutional Animal Care and Use Committee of the University of Missouri and were conducted according to the NIH Guide for the Care and Use of Laboratory Animals. C57BL/6J inbred mice (stock no. 000664) were obtained from Jackson Laboratory, and outbred CD-1 mice (stock no. 022) were purchased from Charles River. Mice were housed in the vivarium of Division of Animal Science at University of Missouri under 10 hours dark and 14 hours light cycles.

Prepubertal 3 to 4 weeks old C57BL/6J were superovulated by i.p. injection of 5 IU Pregnant Mare Serum Gonadotropin (ProSpec, HOR-272) at 1300 hours followed by 5 IU Human Chorionic Gonadotropin (hCG, Sigma, CG5 5000 IU) i.p. injection after 48 hours. These females were placed with fertile C57BL/6J males after the hCG injection. The following day morning, plugged C57BL/6J were euthanized and zygotes were collected, and the cumulus cells were removed with 10 IU/ml hyaluronidase (Sigma, 385931) in M2 media (Millipore Sigma, MR-051-F). Pronuclei stage zygotes were selected for electroporation. On the day of electroporation, adult (8–10 weeks old) CD-1 females on proestrus determined by vaginal smear were placed with tested vasectomized CD-1 males and used as recipients for electroporated C57BL/6 embryos.

2.2 Guide RNA design

A pair of guide RNAs was designed using freeware from Integrated DNA Technologies (IDT) (https://www.idtdna.com/site/order/designtool/index/CRISPR_SEQUENCE) that are unique in the genome to avoiding any predicted off-target effects. The 20 nucleotide plus PAM sequence ALT-R® CRISPR-Cas9 crRNAs (Guides) were purchased from Integrated DNA Technologies. Guide RNAs for *Prss28* were selected on second exon after the start codon on exon 2 (GAACACGGTACTTTCCAGACAGG) and on exon 4 (TCGACTCCACTGACCAGTGTTGG) (Figure 1). Guide RNAs for *Prss29* were selected right before the start codon on intron 1 (TATATATTGAGGCACAAGGGTGG) and another was located on exon 4 (ACACGGATCCGAAAGACTGATGG).

2.3 Ribonucleoprotein (RNP) assembly

The RNP assembly was performed just before electroporation according to Nepagene (NEPA21) recommended protocol for zygote electroporation. ALT-R® CRISPR-Cas9 tracrRNAs (Catalog # 1072523) and ALT-R® S.p. Cas9 Nuclease V3 (Catalog # 1081058) were purchased from IDT. First, tracRNA and each of the two crRNA for a gene were mixed at the 100 μM concentration each with nuclease free water and crRNA:tracRNA duplex was made by annealing the mixture on a thermal cycler at 95°C for 5 min. The duplex mix was then cooled to room temperature. RNP complex for each targeted gene was made of crRNA:tracRNA duplex (6 μM final) and Cas9 Nuclease (1.2 μM final) constituted in in a total volume of 60 μl with Opti-MEM (ThermoFisher, 31985070) and incubated at room temperature for 20 min. Fifty (50) μl RNP mix was used for electroporation.

2.4 Electroporation of pronuclear-stage embryos

We applied electroporation with repeated pulses to first pore the zona pellucida and then transfered RNPs intracellularly by NEPA 21 electroporator (NEPA GENE Co. Ltd., Chiba, Japan). A glass chamber with 8 mm gap platinum plate electrodes (NEPA GENE Co. Ltd, CUY505P5,) was filled with 50 μl of RNPs in Opti-MEM. The impedance was adjusted to 0.5 kΩ. Between 50 and 80 zygotes were aligned in the center line of the chamber, avoiding contacts between zygotes. Electroporation program was set to 225 V, 2 msec pulse length, 50 msec pulse interval, 4 rounds of pulses, 10% decay rate and + polarity for the poring pulse and 20V, 50 msec pulse length, 50 msec pulse interval, 5 rounds of pulses, 40% decay rate and ± polarity for the transfer pulse. After the electroporation, embryos were

washed and transferred in EmbryoMax Advanced KSOM Embryo Media (Millipore Sigma, MR-101-D).

2.5 Embryo culture, transfer and genotyping

Intact 25–30 zygotes were placed in a 30 μl advanced KSOM droplets in petri dish (Corning, 351008) covered with mineral oil (Irvine Scientific, 9305) and incubated overnight under 5% CO_2 at 37°C. Embryos that developed to two cell stage in next day were selected. Pseudo pregnant CD-1 females that were mated with vasectomized males were anesthetized under isoflurane and of 8–10 two cell stage embryos were surgically placed in each oviduct at the bulging near the first coiling from the infundibulum, directing towards the ampulla. Pregnancy was monitored and after the pups were delivered, tail snips were taken before weaning age to isolate the genomic DNA. High quality DNA was purified using Gentra Puregene Mouse Tail Kit (Quiagen, 158267) and PCR amplification was performed with sequencing primer set (Supplemental Table 1) that encompass the targeted loci of the gene. The DNA product corresponding to the mutant band in the gel was purified with Qiaquick Gel Extraction Kit (Qiagen 28704) and Sanger sequencing was performed at the DNA core of University of Missouri. The mutant founder mice were back crossed, and germline transmission was confirmed in F1 pups with genotyping primers (Supplemental Table 1). Regular genotyping was performed in tail snips using a rapid KOH-EDTA digestion method.

2.6 Fertility test

Male and female Prss28, Prss29 and Prss28/Prss29 null matings were setup and monitored for six months.

2.7 Histology and immunofluorescence analyses

Vaginal smearing was performed on wild type, *Prss28* null and *Prss29* null adult females to detect female mice in proestrus. Uteri were harvested, placed in chilled heptane on dry ice and embedded in OCT media (Fisher, 22363554). The uteri were cryosectioned at 6 μM thickness, mounted on Superfrost Plus microscope slides (Fisher, 22037246), and stored at −20°C. Slides with tissue sections were dried at room temperature for 10 min and fixed in ice cold methanol (Fisher, A452) for 10 min. Slides were washed thrice (10 min each) with PBS and antigen retrieval was performed in boiling reveal decloaker solution (BioCare Medical, RV1000M) for 20 minutes and left to cool. The slides were then washed thrice with PBS and blocked with 10% normal goat serum (Life Technologies, 50062Z) for 1 h. Sections were then incubated with a cocktail of primary antibodies to Cytokeratin 8 (TROMA-1; 1:50 dilution of rat monoclonal, University of Iowa Developmental Studies Hybridoma Bank) and FOXA2 (1:400 dilution, Abcam, ab 108422) in 10% normal goat serum overnight at 4°C. After thoroughly washing thrice (PBS for 10 min each), a cocktail of Alexa Fluor conjugated secondary goat anti-rat and anti-rabbit antibodies (1:400 dilution of Invitrogen A-11006 and A-21429) in PBS containing 1% BSA was applied to each section for 1 h at room temperature. After washing thrice (10 min each) with PBS, nuclei were stained for 5 min with Hoechst 33342 (2 μg/ml; Life Technologies H3570). A final wash was performed with water twice (5 min each). Fluoromount-G (ThermoFisher, 495802) mounting media was placed on each section before affixing a coverslip that was sealed with nail polish. Processed tissue sections were inspected for fluorescence and images

recorded with a Leica DM5500 B upright microscope using the Leica Application Suite X (LAS X). Of note, gland number was quantified in 40 non-sequential sections of proestrus uteri from WT, *Prss28* null and *Prss29* null mice.

2.8 qRT-PCR

Total RNA was extracted from proestrus uteri using TRIzol reagent (Thermo Fisher, AM9738). Total RNA (1 μg) was used to synthesize cDNAs for each sample using a High-Capacity cDNA Reverse Transcription Kit (Thermo Fisher, 18064014). The cDNA was diluted ten times with water, and subjected to quantitative reverse transcriptase quantitative PCR (qRT-PCR) to estimate mRNA levels. qRT-PCR primer sequences are presented in Supplemental Table 1. Real-time PCR amplification of cDNAs was carried out in a reaction mixture (10 μL) containing SsoAdvanced Universal SYBR Green Supermix (Bio-Rad, 1725274) and primers (250 nM each). The delta delta Ct method was used for relative quantification of the amount of mRNA for each sample normalized to 18S RNA.

2.9 Statistical analyses

Student's t-test was applied to compare the litter size to the controls. One-way analysis of variance followed by Tukey's post hoc test was applied to compare gene expression differences within each line of mice.

3 Results

3.1 Generation of *Prss28* null mice

CRISPR-Cas9 genome-editing was used to generate targeted mutations. The *Prss28* gene has six exons and two guides were used to target exon 2 and exon 4. The coding sequence starts from the second exon of the gene. The first guide created a DNA break in the first intron at 138 bases upstream of the start codon in exon 2. The second guide created a cut in the fourth exon right at the PAM junction of the guide RNA (Figure 1). The combination of both guides created a deletion of 876 basepairs that encompassed the start codon of the gene (Figure 1). Germline transmission was confirmed in the progeny by genotyping (Supplemental Figure 1). Breeding was performed with heterozygous males and females to create *Prss28* null mice.

3.2 Generation of *Prss29* null mice

The *Prss29* gene also has six exons and the coding sequence starts with the second exon. Two guides were designed to target the first intron and exon 2 boundary and exon 4. The first guide created a break in the first intron 18 bases upstream of the start codon, and the second guide cut 20 bases downstream of the beginning of the fourth exon. This approach created a large deletion of 627 basepairs in the gene (Figure 1). Interestingly, sequencing of PCR products found that a GA sequence was inserted randomly during the repair. After confirming germline transmission in progeny (Supplemental Figure 1), *Prss29* null mice were generated by breeding heterozygous males and females.

3.3 Fertility characterization of the mutant mice

Heterozygous 8 week old females and 3 month old males were setup in cages and breeding was monitored for 6 months. Genotyping with specific primer sets (Supplemental Table 1) was used to identify wild type (WT; +/+), heterozygous (+/−) and null (−/−) pups. As illustrated in Figure 2A, the genotypic distribution of pups from *Prss28* and *Prss29* heterozygote matings displayed Mendelian inheritance. Pups of all genotypes in *Prss28* and *Prss29* litters survived to weaning and reached sexual maturity.

Next, a breeding trial was conducted to compare the reproductive performance of *Prss28* and *Prss29* mutant lines to WT controls. There was no difference (P>0.10) in the litter size in the null-null matings of *Prss28* (6.1 ± 1.8) and *Prss29* (6.1 ± 1.9) mice as compared to the WT-WT matings (6.0 ± 1.3) (Figure 2B). Since there was no obvious litter size phenotype in the females of both *Prss28* and *Prss29* null genotype, a double null genotype female was generated by crossing *Prss28* null and *Prss29* null mice to eliminate any functional redundancy and compensation of these two genes. When the double homozygote *Prss28* and *Prss29* mutant females were bred with WT males, the litter size of *Prss28/Prss29* null-null matings (5.9 ± 2.4) was not different (P>0.01) than WT-WT matings (Figure 2B).

3.4 Uterine histology

Uteri of WT, *Prss28* and *Prss29* null females were collected at two months of age during proestrus phase of the estrous cycle, as those genes are abundantly expressed at that stage (O'Sullivan, Rancourt, et al., 2001). As illustrated in Figure 3A, the proestrus uteri of adult *Prss28* and *Prss29* null females displayed a normal histoarchitecture similar to WT uteri. The number of FOXA2 positive glands were not different (P>0.10) in the uteri of WT, *Prss28*, and *Prss29* null females (Figure 3B).

3.5 Uterine gene expression

As summarized in Figure 4, *Prss28* mRNA was undetectable in the proestrus Prss28 null uteri, and *Prss29* mRNA was not detected in proestrus Prss29 null uteri as expected. *Prss28* and *Prss29* was not altered in any genotypes of the Prss29 and Prss28 lines, respectively.

4. Discussion

Uterine glands and, by inference, their secretions are indispensable for embryo implantation and pregnancy success (Dhakal et al., 2015; Filant, Zhou, & Spencer, 2012; Kelleher, Burns, Behura, Wu, & Spencer, 2016; Kelleher et al., 2018; Kelleher et al., 2017). The FOXA2 transcription factor is specifically expressed in the GE of the endometrium and has pleiotropic effects on gland development and adult uterine function. Utilizing stage and cell-type specific models of FOXA2 deficiency, we previously discovered that *Lif* is not expressed in the absence of FOXA2. LIF is a critical gland specific cytokine expressed in response to nidatory estrogen and is required for embryo implantation in mice (Stewart et al., 1992). Supplementation of recombinant LIF was able to rescue pregnancy in adult FOXA2 cKO mice that contained glands (Kelleher et al., 2018; Kelleher et al., 2017), however there were notable effects on the transcriptome of the decidua as well as differences in fetoplacental growth (Dhakal et al., 2020). Integration with published data identified

Prss28 and *Prss29* as the topmost differentially regulated genes in LIF-replaced FOXA2-deficient mice that are explicitly expressed in the uterine glands (Kelleher et al., 2017).

Utilizing CRISPR-Cas9 genome-editing we generated individual knockouts of *Prss28* and *Prss29* and characterized their fertility. Breeding trials consisting of heterozygous males and females generated normal litter sizes with the expected genotypes with normal patterns of Mendelian inheritance. Similarly, knockout breedings produced litter sizes comparable to wildtype and heterozygous breeding controls. As expected, there was no difference in the uterine histoarchitecture in *Prss28* and *Prss29* null mice when compared to WT. Further, *Prss28* and *Prss29* null uteri appeared normal from the perspective of gene expression of *Esr1*, *Pgr*, *Foxa2*, and *Spink1*. Based on the similarity in expression of *Prss28* and *Prss29*, as well as their 46% similarity in DNA sequence, conserved histidine-aspartic acid-serine active site moieties, and highly conserved 5′-UTRs, we hypothesized that *Prss28* and *Prss29* may be functionally redundant (O'Sullivan et al., 2004; Tang & Rancourt, 2005). To circumvent the possibility of compensation, we crossed the two lines and created *Prss28* and *Prss29* double homozygous null females. When double knockout females were bred with fertile males there was no deviation from normal litter size. Thus, *Prss28* and *Prss29* are dispensable for fertility and do not have a role embryo development or uterine functions for pregnancy.

A potentially important consideration is that the experiments in this study were conducted in standard vivarium where the hygiene is tightly controlled. Of note, proteases are involved in host defense mechanisms involved in the maintenance of pregnancy (Salamonsen & Nie, 2002). During infection, dysregulation of protease activation can result aberrant processing of inflammatory mediators, altering their function in vivo, and ultimately causing excessive inflammation and damage to cells and tissue systems leading to increased morbidity and mortality (Marshall, Finlay, & Overall, 2017). Our studies did not explore the role of *Prss28* and *Prss29* in mice challenged with pathogens commonly found in human reproductive tract (Reese et al., 2016). Thus, a pregnancy phenotype could emerge in *Prss28* and *Prss29* knockout mice in a more natural setting.

In conclusion, we utilized a Crispr-Cas9 gene editing approach to directly test the function of two FOXA2-dependent progesterone-induced genes in female reproduction. *Prss28* and *Prss29* single and double null females are fertile and exhibit no overt fertility phenotype. Thus, we conclude that Prss28 and Prss29 are dispensable for reproduction under standard husbandry conditions.

Supplementary Material

Refer to Web version on PubMed Central for supplementary material.

Acknowledgments

We thank Chaman Ranjit for assistance in laboratory support, John D'Alessandro for mouse husbandry support, and Andrew Kelleher for editing and input.

Funding information

This work was funded, in part, by the National Institutes of Health/National Institute of Child Health and Human Development grant R01 HD096266.

References

Arora R, Fries A, Oelerich K, Marchuk K, Sabeur K, Giudice LC, & Laird DJ (2016). Insights from imaging the implanting embryo and the uterine environment in three dimensions. Development, 143(24), 4749–4754. doi:10.1242/dev.144386 [PubMed: 27836961]

Bhatt H, Brunet LJ, & Stewart CL (1991). Uterine expression of leukemia inhibitory factor coincides with the onset of blastocyst implantation. Proc Natl Acad Sci U S A, 88(24), 11408–11412. doi:10.1073/pnas.88.24.11408 [PubMed: 1722331]

Burton GJ, Watson AL, Hempstock J, Skepper JN, & Jauniaux E (2002). Uterine glands provide histiotrophic nutrition for the human fetus during the first trimester of pregnancy. J Clin Endocrinol Metab, 87(6), 2954–2959. doi:10.1210/jcem.87.6.8563 [PubMed: 12050279]

Chen JR, Cheng JG, Shatzer T, Sewell L, Hernandez L, & Stewart CL (2000). Leukemia inhibitory factor can substitute for nidatory estrogen and is essential to inducing a receptive uterus for implantation but is not essential for subsequent embryogenesis. Endocrinology, 141(12), 4365–4372. doi:10.1210/endo.141.12.7855 [PubMed: 11108244]

Chen W, Han BC, Wang RC, Xiong GF, & Peng JP (2010). Role of secretory protease inhibitor SPINK3 in mouse uterus during early pregnancy. Cell Tissue Res, 341(3), 441–451. doi:10.1007/s00441-010-1013-5 [PubMed: 20623140]

Cooke PS, Ekman GC, Kaur J, Davila J, Bagchi IC, Clark SG, … Bartol FF (2012). Brief exposure to progesterone during a critical neonatal window prevents uterine gland formation in mice. Biol Reprod, 86(3), 63. doi:10.1095/biolreprod.111.097188 [PubMed: 22133692]

Daikoku T, Ogawa Y, Terakawa J, Ogawa A, DeFalco T, & Dey SK (2014). Lactoferrin-iCre: a new mouse line to study uterine epithelial gene function. Endocrinology, 155(7), 2718–2724. doi:10.1210/en.2014-1265 [PubMed: 24823394]

Dhakal P, Kelleher AM, Behura SK, & Spencer TE (2020). Sexually dimorphic effects of forkhead box a2 (FOXA2) and uterine glands on decidualization and fetoplacental development. Proc Natl Acad Sci U S A, 117(38), 23952–23959. doi:10.1073/pnas.2014272117 [PubMed: 32900950]

Dhakal P, Rumi MA, Kubota K, Chakraborty D, Chien J, Roby KF, & Soares MJ (2015). Neonatal Progesterone Programs Adult Uterine Responses to Progesterone and Susceptibility to Uterine Dysfunction. Endocrinology, 156(10), 3791–3803. doi:10.1210/en.2015-1397 [PubMed: 26204463]

Filant J, Lydon JP, & Spencer TE (2014). Integrated chromatin immunoprecipitation sequencing and microarray analysis identifies FOXA2 target genes in the glands of the mouse uterus. FASEB J, 28(1), 230–243. doi:10.1096/fj.13-237446 [PubMed: 24025729]

Filant J, & Spencer TE (2013). Endometrial glands are essential for blastocyst implantation and decidualization in the mouse uterus. Biol Reprod, 88(4), 93. doi:10.1095/biolreprod.113.107631 [PubMed: 23407384]

Filant J, Zhou H, & Spencer TE (2012). Progesterone inhibits uterine gland development in the neonatal mouse uterus. Biol Reprod, 86(5), 146, 141–149. doi:10.1095/biolreprod.111.097089 [PubMed: 22378759]

Fouladi-Nashta AA, Jones CJ, Nijjar N, Mohamet L, Smith A, Chambers I, & Kimber SJ (2005). Characterization of the uterine phenotype during the peri-implantation period for LIF-null, MF1 strain mice. Dev Biol, 281(1), 1–21. doi:10.1016/j.ydbio.2005.01.033 [PubMed: 15848385]

Gray CA, Burghardt RC, Johnson GA, Bazer FW, & Spencer TE (2002). Evidence that absence of endometrial gland secretions in uterine gland knockout ewes compromises conceptus survival and elongation. Reproduction, 124(2), 289–300. [PubMed: 12141942]

Gray CA, Taylor KM, Ramsey WS, Hill JR, Bazer FW, Bartol FF, & Spencer TE (2001). Endometrial glands are required for preimplantation conceptus elongation and survival. Biol Reprod, 64(6), 1608–1613. doi:10.1095/biolreprod64.6.1608 [PubMed: 11369585]

Jeong JW, Kwak I, Lee KY, Kim TH, Large MJ, Stewart CL, … DeMayo FJ (2010). Foxa2 is essential for mouse endometrial gland development and fertility. Biol Reprod, 83(3), 396–403. doi:10.1095/biolreprod.109.083154 [PubMed: 20484741]

Jinek M, Chylinski K, Fonfara I, Hauer M, Doudna JA, & Charpentier E (2012). A programmable dual-RNA-guided DNA endonuclease in adaptive bacterial immunity. Science, 337(6096), 816–821. doi:10.1126/science.1225829 [PubMed: 22745249]

Kelleher AM, Behura SK, Burns GW, Young SL, DeMayo FJ, & Spencer TE (2019). Integrative analysis of the forkhead box A2 (FOXA2) cistrome for the human endometrium. FASEB J, 33(7), 8543–8554. doi:10.1096/fj.201900013R [PubMed: 30951376]

Kelleher AM, Burns GW, Behura S, Wu G, & Spencer TE (2016). Uterine glands impact uterine receptivity, luminal fluid homeostasis and blastocyst implantation. Sci Rep, 6, 38078. doi:10.1038/srep38078 [PubMed: 27905495]

Kelleher AM, DeMayo FJ, & Spencer TE (2019). Uterine Glands: Developmental Biology and Functional Roles in Pregnancy. Endocr Rev, 40(5), 1424–1445. doi:10.1210/er.2018-00281 [PubMed: 31074826]

Kelleher AM, Milano-Foster J, Behura SK, & Spencer TE (2018). Uterine glands coordinate on-time embryo implantation and impact endometrial decidualization for pregnancy success. Nat Commun, 9(1), 2435. doi:10.1038/s41467-018-04848-8 [PubMed: 29934619]

Kelleher AM, Peng W, Pru JK, Pru CA, DeMayo FJ, & Spencer TE (2017). Forkhead box a2 (FOXA2) is essential for uterine function and fertility. Proc Natl Acad Sci U S A, 114(6), E1018–E1026. doi:10.1073/pnas.1618433114 [PubMed: 28049832]

Marshall NC, Finlay BB, & Overall CM (2017). Sharpening Host Defenses during Infection: Proteases Cut to the Chase. Mol Cell Proteomics, 16(4 suppl 1), S161–S171. doi:10.1074/mcp.O116.066456 [PubMed: 28179412]

O'Sullivan CM, Liu SY, Karpinka JB, & Rancourt DE (2002). Embryonic hatching enzyme strypsin/ISP1 is expressed with ISP2 in endometrial glands during implantation. Mol Reprod Dev, 62(3), 328–334. doi:10.1002/mrd.10142 [PubMed: 12112596]

O'Sullivan CM, Liu SY, Rancourt SL, & Rancourt DE (2001). Regulation of the strypsin-related proteinase ISP2 by progesterone in endometrial gland epithelium during implantation in mice. Reproduction, 122(2), 235–244. [PubMed: 11467974]

O'Sullivan CM, Rancourt SL, Liu SY, & Rancourt DE (2001). A novel murine tryptase involved in blastocyst hatching and outgrowth. Reproduction, 122(1), 61–71. doi:10.1530/rep.0.1220061 [PubMed: 11425330]

O'Sullivan CM, Ungarian JL, Singh K, Liu S, Hance J, & Rancourt DE (2004). Uterine secretion of ISP1 & 2 tryptases is regulated by progesterone and estrogen during pregnancy and the endometrial cycle. Mol Reprod Dev, 69(3), 252–259. doi:10.1002/mrd.20169 [PubMed: 15349836]

Ohmuraya M, Hirota M, Araki M, Mizushima N, Matsui M, Mizumoto T, … Yamamura K (2005). Autophagic cell death of pancreatic acinar cells in serine protease inhibitor Kazal type 3-deficient mice. Gastroenterology, 129(2), 696–705. doi:10.1016/j.gastro.2005.05.057 [PubMed: 16083722]

Playford RJ, & Marchbank T (2020). Pancreatic secretory trypsin inhibitor reduces multi-organ injury caused by gut ischemia/reperfusion in mice. PLoS One, 15(1), e0227059. doi:10.1371/journal.pone.0227059 [PubMed: 31923181]

Ran FA, Hsu PD, Wright J, Agarwala V, Scott DA, & Zhang F (2013). Genome engineering using the CRISPR-Cas9 system. Nat Protoc, 8(11), 2281–2308. doi:10.1038/nprot.2013.143 [PubMed: 24157548]

Reese TA, Bi K, Kambal A, Filali-Mouhim A, Beura LK, Burger MC, … Virgin HW (2016). Sequential Infection with Common Pathogens Promotes Human-like Immune Gene Expression and Altered Vaccine Response. Cell Host Microbe, 19(5), 713–719. doi:10.1016/j.chom.2016.04.003 [PubMed: 27107939]

Salamonsen LA, & Nie G (2002). Proteases at the endometrial-trophoblast interface: their role in implantation. Rev Endocr Metab Disord, 3(2), 133–143. doi:10.1023/a:1015407012559 [PubMed: 12007290]

Soyal SM, Mukherjee A, Lee KY, Li J, Li H, DeMayo FJ, & Lydon JP (2005). Cre-mediated recombination in cell lineages that express the progesterone receptor. Genesis, 41(2), 58–66. doi:10.1002/gene.20098 [PubMed: 15682389]

Stewart CL (1994). The role of leukemia inhibitory factor (LIF) and other cytokines in regulating implantation in mammals. Ann N Y Acad Sci, 734, 157–165. doi:10.1111/j.1749-6632.1994.tb21743.x [PubMed: 7978912]

Stewart CL, Kaspar P, Brunet LJ, Bhatt H, Gadi I, Kontgen F, & Abbondanzo SJ (1992). Blastocyst implantation depends on maternal expression of leukaemia inhibitory factor. Nature, 359(6390), 76–79. doi:10.1038/359076a0 [PubMed: 1522892]

Tang L, & Rancourt DE (2005). Murine implantation serine proteinases 1 and 2: structure, function and evolution. Gene, 364, 30–36. doi:10.1016/j.gene.2005.07.041 [PubMed: 16257142]

Turpeinen U, Koivunen E, & Stenman UH (1988). Reaction of a tumour-associated trypsin inhibitor with serine proteinases associated with coagulation and tumour invasion. Biochem J, 254(3), 911–914. doi:10.1042/bj2540911 [PubMed: 2461702]

Villacorte M, Suzuki K, Hirasawa A, Ohkawa Y, Suyama M, Maruyama T, … Yamada G (2013). beta-Catenin signaling regulates Foxa2 expression during endometrial hyperplasia formation. Oncogene, 32(29), 3477–3482. doi:10.1038/onc.2012.376 [PubMed: 22945641]

Wang J, Ohmuraya M, Hirota M, Baba H, Zhao G, Takeya M, … Yamamura K (2008). Expression pattern of serine protease inhibitor kazal type 3 (Spink3) during mouse embryonic development. Histochem Cell Biol, 130(2), 387–397. doi:10.1007/s00418-008-0425-8 [PubMed: 18386042]

Yuan J, Deng W, Cha J, Sun X, Borg JP, & Dey SK (2018). Tridimensional visualization reveals direct communication between the embryo and glands critical for implantation. Nat Commun, 9(1), 603. doi:10.1038/s41467-018-03092-4 [PubMed: 29426931]

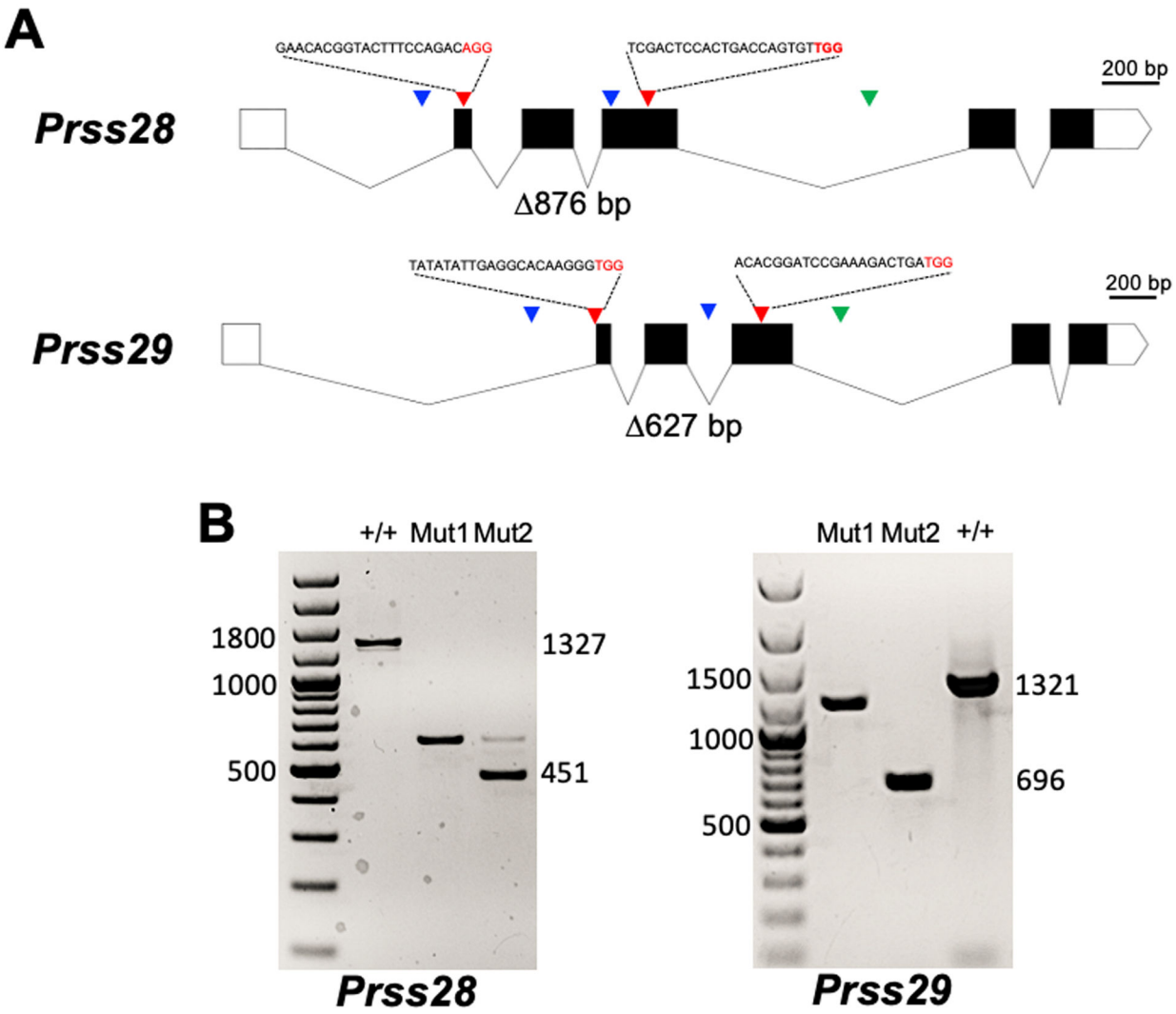

Figure 1.

(A) Schematic representation of *Prss28 and Prss29* gene organization and approach used to generate mutant mice using CRISPR/Cas9 genome editing. The position of guide RNAs is denoted by red triangles along with their sequences. Positions of forward and reverse primers used for genotyping are indicated by blue and green triangles, respectively. (B) PCR was performed on genomic DNA from the tail snips of *Prss28* and *Prss29* F0 generation pups to identify mutant animals. Mutant animal number 2 (Mut2) with Δ876 bp and Δ627 bp deletions in *Prss28* and *Prss29*, respectively, were bred to propagate and establish gene-edited lines.

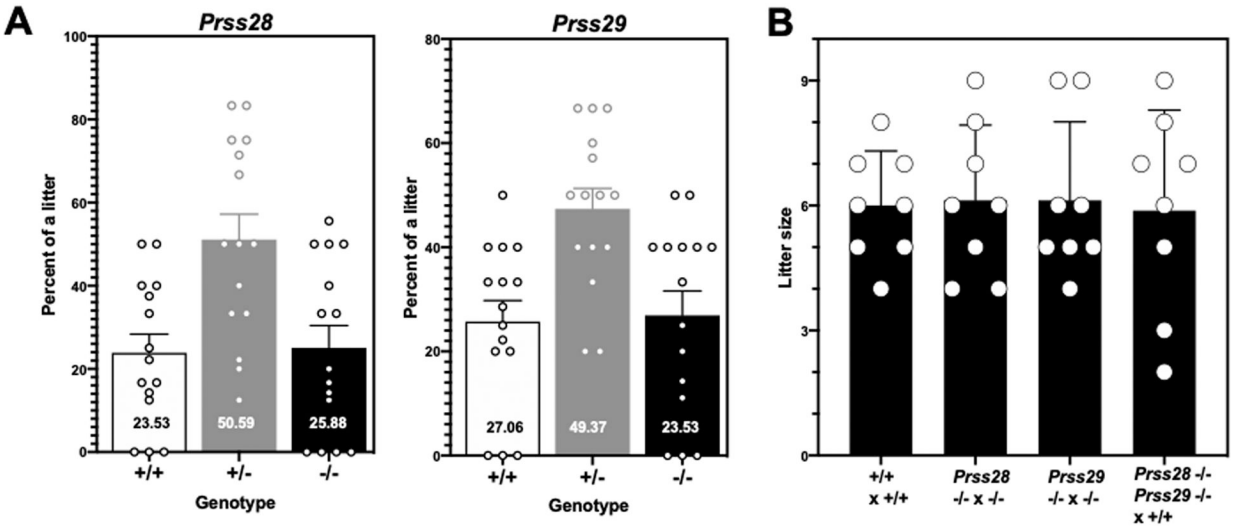

Figure 2.

Aspects of pregnancy outcomes in wild type (WT), *Prss28* null, and *Prss29* null mice. (A) Genotype distribution of pups from *Prss28* and *Prss29* heterozygous male and female matings (n= 15 each). (B) Litter size in matings of wild type (WT), *Prss28* null, *Prss29* null, and *Prss28/Prss29* double null females (n = 8 each). Data is expressed as number of pups per litter.

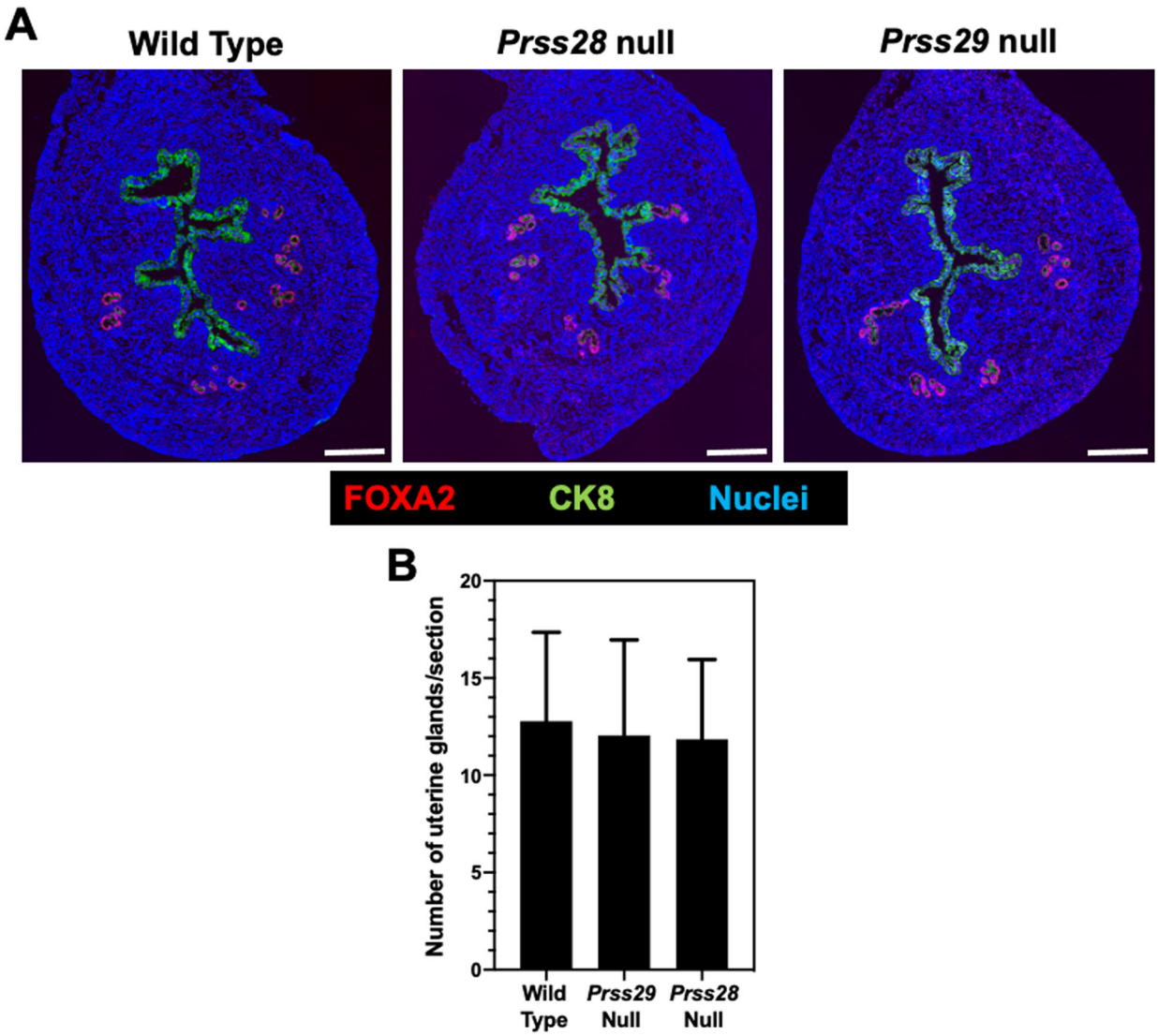

Figure 3.

(A) Uterine histoarchitecture and FOXA2 localization in proestrus uteri from wild type, *Prss28* null, and *Prss29* females at 2 months of age. Bar, 250 μm. (B) Gland number in sections of uteri from proestrus wild type, *Prss28* null and *Prss29* null mice (n = 6 mice per genotype).

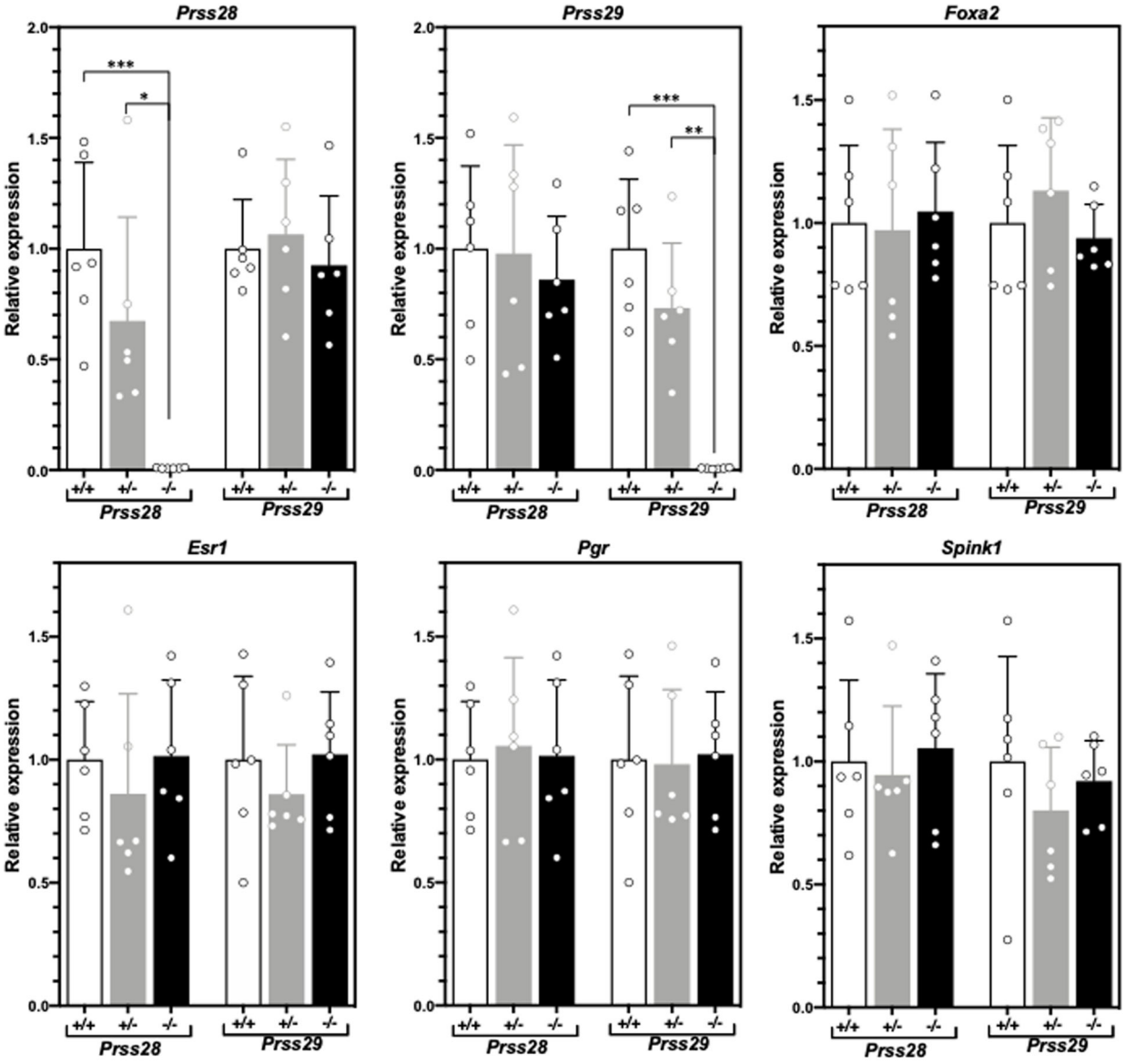

Figure 4.

Effects of *Prss28* and *Prss29* gene deletion on gene expression in the uterus of proestrus mice. Real-time qPCR analysis was conducted using uteri from wild type (+/+), heterozygous (+/−), and null (−/−) mice (n = 5 per genotype). Data are expressed relative to mRNA levels in wild type (+/+) mice. *P<0.01, **P < 0.001, and ***P<0.0001.